

PHASE-TRANSIENT HIERARCHICAL TURBULENCE AS AN ENERGY CORRELATION GENERATOR OF BLAZAR LIGHT CURVES

MITSURU HONDA

Plasma Astrophysics Laboratory, Institute for Global Science, Mie 519-5203, Japan

Draft version February 6, 2020

ABSTRACT

Hierarchical turbulent structure constituting a jet is considered to reproduce energy-dependent variability in blazars, particularly, the correlation between X- and gamma-ray light curves measured in the TeV blazar Markarian 421. The scale-invariant filaments are featured by the ordered magnetic fields that involve hydromagnetic fluctuations serving as electron scatterers for diffusive shock acceleration, and the spatial size scales are identified with the local maximum electron energies, which are reflected in the synchrotron spectral energy distribution (SED) above the near-infrared/optical break. The structural transition of filaments is found to be responsible for the observed change of spectral hysteresis.

Subject headings: BL Lacertae objects: individual (Mrk 421) — galaxies: jets — magnetic fields — radiation mechanisms: nonthermal — turbulence

1. INTRODUCTION

A noticeable feature associated with blazars is that the updated shortest variability timescale reaches a few minutes (e.g., Mrk 421: Cui 2004; Błażejowski et al. 2005), not likely to be reconciled with the light-crossing time at the black hole horizon. One possible explanation for this fact is that small-scale structure does exist in the parsec-scale jet anchored in the galactic core (Honda & Honda 2004). Indeed, in the plausible circumstance that the successive impingement of plasma blobs (ejected from the core) into the jet bulk engenders collisionless shocks, electromagnetic current filamentation (characterized by the skin depth) could be prominent (Medvedev & Loeb 1999). It is known that the merging of smaller filaments leads eventually to accumulation of magnetic energy in larger scales (Honda et al. 2000a; Silva et al. 2003).

Reflecting the self-similar (power law) characteristic in the inertially cascading range, the local magnetic intensity of the self-organized filaments will obey $|\mathbf{B}| \sim B_m(\lambda/d)^{(\beta-1)/2}$, where λ and d reflect the transverse size scale of a filament and the maximum, respectively, $B_m \equiv |\mathbf{B}|_{\lambda=d}$, and β (> 1) corresponds to the filamentary turbulent spectral index. The value of d is limited by the transverse size of jet (or blob size; D). Then, it is reasonable to consider that in fluid timescales, the well-developed coherent fields are sure to actually meet hydromagnetic disturbance independent of the filamentation; that is, the turbulent hierarchy is established (see Fig. 1). The spectral index of the superposed fluctuations [denoted as β' (> 1)] could be different from β , and the correlation length scale is presumably limited by $\sim \lambda$.

At this site, the electrons bound to the local mean fields suffer scattering by the fluctuations, to be diffusively accelerated by the collisionless shocks (see Honda & Honda 2007). When the acceleration and cooling efficiency depend on the spatial size scales, the local maximum energies of accelerated electrons will be identified by λ (§ 2), to be reflected in the synchrotron SED extending to the X-ray region. More interestingly, the spatially inhomogeneous property of particle energetics is expected to cause

the energy-dependent variability of broadband SEDs. Here the naive question arises whether or not this idea is responsible for the observed elusive patterns of energy correlation of light curves (e.g., Takahashi et al. 1996; Fossati et al. 2000a,b; Błażejowski et al. 2005): this is the original motivation of the current work.

In the present simplistic model, light travel time effects would still prevent the detection of variability signatures on timescales shorter than $D/(c\delta_z)$, where $\delta_z = \delta/(1+z)$, and δ , z , and c are the beaming factor of the jet, redshift, and speed of light, respectively. However, if a filamented piece is isolated, having loose causal relation with the dynamics of a bulk region serving as a dominant emitter, an intrinsic rapid variability involved in the subsystem would be viable. Namely, it is inferred that the shorter timescale is at least potentially realized, and observable, unless energetic emissions from such a compact domain are crucially degraded by synchrotron self-absorption and/or $\gamma\gamma$ absorption (e.g., Aharonian 2004). As is, the basic notion of the present model seems to provide a vital clue to settle the debate as to the causality problem incidental to observed rapid variabilities.

In this Letter, I demonstrate that the hierarchical system incorporated with the synchrotron self-Compton (SSC) mechanism accurately generates the time lag of gamma-ray flaring activity behind the X-ray, confirmed in the high-frequency-peaked BL Lac object Mrk 421 (Błażejowski et al. 2005). We address that in general, both lag and lead can appear in X-ray interband correlations, accompanying the structural transition. The major transition history is argued in light of the observed spectral hysteresis patterns. We also work out (B_m, d) , to provide the constraint on the field strength and D that should be compared with those of previous models.

2. AN IMPROVED EMITTER MODEL WITH HIERARCHICAL STRUCTURE

We consider a circumstance in which relativistic shocks propagate through a relativistic jet with the Lorentz factor Γ , such that the shock viewed upstream (jet frame) is weakly to mildly relativistic. Note the relation of $\delta \sim \Gamma$. The overall geometry and relative size scales of the afore-

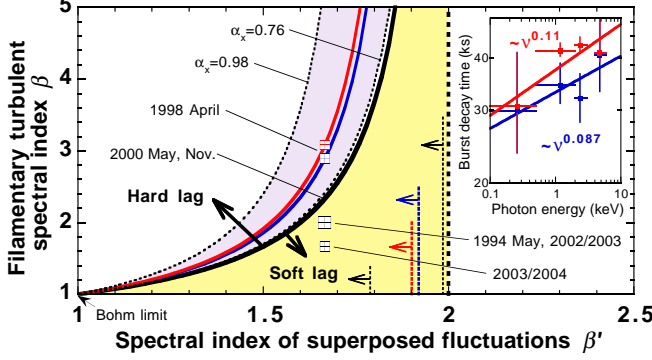


FIG. 2.— Phase diagram of the hierarchical turbulence. The function $\beta_c(\beta')$ (eq. [2]; *thick solid curve*) divides the (β, β') -plane into the two domains that allow soft-lag ($\beta < \beta_c$; *yellow*) and hard-lag ($\beta > \beta_c$) in the X-ray band. The possible phases Φ_2 (2, 5/3) and $\Phi_{5/3}$ (5/3, 5/3) (*large and small marks*, respectively) involve soft-lag, as consistent with the correlations measured in the labeled epochs. The inset shows the power-law fit to two available τ - ν data on 1998 April 21 (for detailed data reduction, see Fossati et al. 2000a), giving the indices of $s = 0.11$ and 0.087 (corresponding colors), which determine $\beta(\beta'; s)$ (*colored curves*) for $\beta' < (s + 2)/(s + 1)$ (*colored arrows*). The characteristic curves lie in a domain (*purple*; β' -range is indicated by thin solid arrows) restricted by the measured X-ray spectral indices (and $p = 1.6$; Fossati et al. 2000b), and give $\beta = 3.1$ and 2.9 (*colored marks*) at $\beta' = 5/3$. For further explanation, see the text.

reasonable fit to the measured ones (at flares) in the mid state (2002–2003) and high state (2004–2005), respectively, of Mrk 421, suggesting $\nu_b \sim 2 \times 10^{14}$ Hz (not shown in figure), as compatible with smaller variability in the ν -range below R band (Błażejowski et al. 2005). Below, we refer to these possible phases $(\beta, \beta') = (2, 5/3)$ and $(5/3, 5/3)$, which satisfy equation (2), as “ Φ_2 ” and “ $\Phi_{5/3}$ ”, respectively. Also, we compare with the detailed data of burst decay time (in 1998; Fossati et al. 2000a). The guideline is given in Figure 2: use is made of the translation of the measured timescale $\propto \nu^s$ to $\beta = [4 - \beta' + s(\beta' - 1)] / [3[2 - \beta' - s(\beta' - 1)]]$. This characteristic curve for $s \simeq 0.1$ indicates $\beta \simeq 3$ at $\beta' = 5/3$, and $\beta > \beta_c$, as consistent with the measured hard lag. For these $\beta = 5/3, 2$, and 3 , we anticipate $(\nu F_\nu)_p \propto \nu_p^{0.8}$, $\nu_p^{0.9}$, and ν_p (for $p \simeq 1.6$; e.g., Macomb et al. 1995), amenable to the full X-ray data analysis of Mrk 421 flares (Tramacere et al. 2007).

Let us now estimate the time lag of a soft energy band $\epsilon_L (> h\nu_b; h$ is the Planck constant) behind a hard band $\epsilon_H (< h\nu_c)$ by $\Delta\tau = \tau(\epsilon_L) - \tau(\epsilon_H)$. Here it is instructive to note the relation of $(\lambda_c <) \lambda(\epsilon_H) < \lambda(\epsilon_L) (< d)$. Using the expression of ν_b (eliminating $\xi^{3/2}d^{-1}$), we obtain

$$\Delta\tau = 1.8 \delta_{50}^{-1/2} B_{m,10}^{-3/2} \nu_{b,14}^{-3/7} \epsilon_{L,1}^{-1/14} \eta_{-1} \text{ hr} \quad (3)$$

for the structural phase Φ_2 , where $\nu_{b,14} = \nu_b/10^{14}$ Hz, $\eta_{-1} = [1 - (\epsilon_L/\epsilon_H)^{1/14}]/10^{-1}$, and $\epsilon_{L,1} = \epsilon_L/1$ keV. Concerning the validity, it has been checked that, e.g., for a soft-lag episode (in 1994 May; Takahashi et al. 1996), the measured time lag plotted against ϵ_L could be more naturally fitted by the function (3) of $\Delta\tau(\epsilon_L, \epsilon_H)$ (given $\epsilon_H \simeq 4 - 5$ keV for *ASCA*), rather than the function of $\sim \epsilon_L^{-1/2}[1 - (\epsilon_L/\epsilon_H)^{1/2}]$ for the homogeneous ($\sigma = 0$) model.

3.2. X/Gamma-Ray Cross-Band Correlation

The interband correlation property is reflected in the cross-band correlation between X- and gamma-rays, provided the SSC mechanism as a dominant gamma-ray emitter (e.g., Maraschi et al. 1992; Dermer & Schlickeiser 1993). Along the heuristic (time independent) manner, we suppose $\gamma \sim \gamma^*$ for scattering electrons, and examine the correlation between an X-ray band ϵ_x (compared to ϵ_H) and gamma-ray band ϵ_γ susceptible to the inverse Comptonization of low-energy synchrotron photons (with ϵ_L). Here we focus on the feasible, Thomson regime of $(\epsilon_L/\delta_z)\gamma^* < m_e c^2$; note that using the expression of $\gamma^*[\lambda(\epsilon_L)]$ (§ 3.1), this range can be written as $\epsilon_L < \delta_{50}[B_{m,10}^2(\xi_{-4}^{3/2}d_{16}^{-1})]^{2/23}$ keV (for Φ_2). The Lorentz factor of the electrons that execute the boost of $\epsilon_\gamma/\epsilon_L = (\gamma^*)^2$ is denoted as $\gamma_s^* = (\epsilon_\gamma/\delta_z h\nu_0)^{1/4}[\lambda(\epsilon_L)/d]^{-(\beta-1)/8}$. Then, simply estimating $\Delta\tau_{\gamma x} = \tau[\epsilon_\gamma/(\gamma_s^*)^2] - \tau(\epsilon_x)$ (> 0 , for $\beta < \beta_c$) would be adequate for the present purpose. For convenience, one may eliminate ϵ_L from γ_s^* [transform $\lambda(\epsilon_L)$ into $\lambda(\epsilon_\gamma)$], and adopt the positive soft-lag representation of $\Delta\tau_{x\gamma} (= -\Delta\tau_{\gamma x})$, so that the negative sign indicates gamma-ray lag. Again using ν_b , we find for Φ_2

$$\Delta\tau_{x\gamma} = -1.7 \delta_{50}^{-5/32} B_{m,10}^{-7/8} \nu_{b,14}^{-7/16} \epsilon_{\gamma,1}^{-1/32} \eta_{\gamma x,-1} \text{ days}, \quad (4)$$

where $\eta_{\gamma x,-1} = \{1 - 0.79\epsilon_{x,25}^{-1/14}[(\epsilon_{\gamma,1}\delta_{50}B_{m,10})]^{1/2} \times \nu_{b,14}^{1/7}\}^{1/16}/10^{-1}$, $\epsilon_{\gamma,1} = \epsilon_\gamma/1$ TeV, and $\epsilon_{x,25} = \epsilon_x/25$ keV. The simultaneous equations (3) and (4) contain the solutions (δ, B_m) , for given observable quantities ν_b and $(\Delta\tau, \Delta\tau_{x\gamma})$, as well as $(\epsilon_L, \epsilon_H; \epsilon_x, \epsilon_\gamma)$ inherent in detectors.

In Figure 3 (*top*) for $\nu_{b,14} = 2$, $\Delta\tau = 1$ hr, and $(\epsilon_{L,1}, \epsilon_L/\epsilon_H; \epsilon_{x,25}) = (1, 0.2; 1)$, compared to Mrk 421 ($z = 0.031$) measurements (Takahashi et al. 1996; Błażejowski et al. 2005), the self-consistent numerical solution δ is plotted against $\Delta\tau_{x\gamma}$, given ϵ_γ that covers a gamma-ray band associated with the Whipple observation (Catanese & Weekes 1999). For the allowed domain of $\delta > 1$ (Piner et al. 1999), a typical TeV range of $\epsilon_{\gamma,1} \simeq 1 - 2$ (susceptible to the significant variation in the mid state) is found to a priori restrict the domain of the observable $-\Delta\tau_{x\gamma}$ to 1.4–2.2 days. Surprisingly, this quantitatively agrees with $\Delta\tau_{x\gamma} = -1.8 \pm 0.4$ days that has been revealed by multiband monitoring in the 2002/2003 season (Błażejowski et al. 2005). In order to solidify the argument, the solutions for the high state with $\Phi_{5/3}$ have also been sought. The results show that the upper bound of $-\Delta\tau_{x\gamma}$, at which δ diverges, shifts (from 2.2 days) to 1.7 days and the Whipple coverage $\epsilon_{\gamma,1} < 10$ restricts to $-\Delta\tau_{x\gamma} > 0.7$ days; these combination yields $-\Delta\tau_{x\gamma} \simeq 0.7 - 1.7$ days. This is certainly compatible with the measured $\Delta\tau_{x\gamma} = -1.2 \pm 0.5$ days (in the 2003/2004 season; for the significance, see Błażejowski et al. 2005).

3.3. Hysteresis Reversal via Structural Transition

From the view point of activity history, it is claimed that, involving the fluctuations with a common $\beta' = 5/3$, the coherent structure, at least, in the dominant emission region has been in the $\beta = 2$ phase (1994 May; Takahashi et al. 1996), $\beta = 3$ (1998 April; Fossati et al. 2000a,b), an intermediate phase around $\beta = 7/3$ (2000 May and November; Sembay et al. 2002),

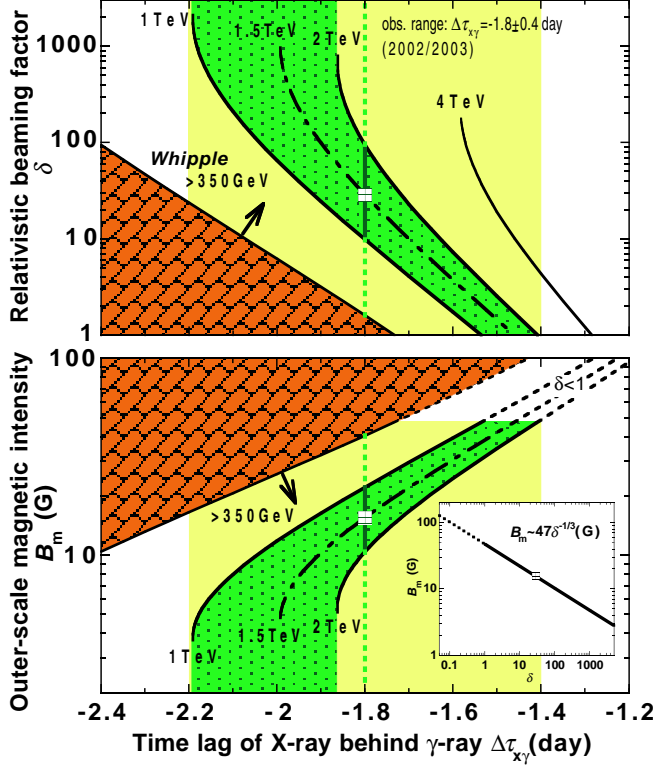


FIG. 3.— Beaming factor δ (top) and maximum field strength B_m (bottom) vs. the time lag of X-ray behind gamma-ray $\Delta\tau_{X\gamma}$ (< 0 means gamma-ray lag) for a given gamma-ray band ϵ_γ (labeled) as a parameter. The horizontal axes are common in the panels. The correlation is taken between $\epsilon_x = 25$ keV and $\epsilon_\gamma \geq 350$ GeV compared to an *RXTE* band and coverage of the Whipple 10m telescope (brick-like shaded area indicates the prohibited domains), respectively. The hatched bands (green) indicate the allowed domains for $\epsilon_\gamma = 1 - 2$ TeV and $\delta > 1$, which cover the measured $\Delta\tau_{X\gamma} = -1.8 \pm 0.4$ days (yellow) and give $\delta = 10 - 92$ and $B_m = 10 - 22$ G at $\Delta\tau_{X\gamma} = -1.8$ days (deep green bars; say, $\delta = 29$ and $B_m = 16$ G [marks] for $\epsilon_\gamma = 1.5$ TeV [dot-dashed curves]). The inset in the bottom panel shows the B_m - δ relation independent of ϵ_γ .

$\beta = 2$ (2002/2003 season; Błażejowski et al. 2005), and $\beta = 5/3$ (2003/2004 season; Błażejowski et al. 2005), to give rise to a hard and soft X-ray lag for $\beta \geq \beta_c = 7/3$, respectively, and no lag for $\beta = \beta_c$, as consistent with the observed correlation properties in each epoch (Fig. 2). At this juncture, the confirmed reversal between clockwise (Takahashi et al. 1996; Rebillot et al. 2006) and anticlockwise (Fossati et al. 2000b) hysteresis loops in the flux-spectral index plane is ascribed to the phase transition between $\beta < \beta_c$ and $> \beta_c$, respectively. Physically, the likely $\beta = 2$ is associated with the prominence of filamentation (Montgomery & Liu 1979). The smaller $\beta = 5/3$ in a high state arguably reflects strong structural deformation, while the larger $\beta = 3$ can be interpreted as the dual-cascade phase of two-dimensional turbulence (e.g., Krommes 2002 and references therein) transverse to pronounced filaments (Honda et al. 2000b).

4. DISCUSSION AND CONCLUDING REMARKS

The practical formula that constrains magnetic field strength is readily obtained from equation (3), and in parallel, one for $\Phi_{5/3}$ can be derived as well. We find the

outcome that for Φ_2 and $\Phi_{5/3}$, B_m must satisfy

$$B_m \delta_z^{1/3} = \begin{cases} 54 \nu_{b,14}^{-2/7} (\Delta\tau^{-1} \epsilon_{L,1}^{-1/14} \eta_{-1})^{2/3} \text{ G}, \\ 33 \nu_{b,14}^{-2/9} (\Delta\tau^{-1} \epsilon_{L,1}^{-1/6} \eta_{-1}^*)^{2/3} \text{ G}, \end{cases} \quad (5)$$

respectively, where $\eta_{-1}^* = [1 - (\epsilon_L/\epsilon_H)^{1/6}]/10^{-1}$ and $\Delta\tau$ is in hours. In Figure 3 (bottom), we plot the self-consistent solution B_m (against $\Delta\tau_{X\gamma}$; corresponding to δ - $\Delta\tau_{X\gamma}$ in Fig. 3 [top]) that obeys equation (5) for Φ_2 (inset) with the same parameter values as the top panel. We see that the observed $\delta > 1$ (Piner et al. 1999) provides the constraint for which local magnetic intensity ($|\mathbf{B}|$) never exceeds 47 G for Φ_2 (51 G for $\Phi_{5/3}$). Whereas a mean magnetic intensity \bar{B} is not well defined within the present framework, the obtained scaling of $B_{m,10} \delta^{1/3} \simeq 5$ seems to be reconciled with the conventional $\bar{B} \delta^{1/3} \simeq 0.1 - 1$ G derived from fitting a variety of homogeneous SSC models to the measured broadband SEDs (e.g., Ghisellini et al. 1998; Tavecchio et al. 1998; Krawczynski et al. 2001).

In turn, the quantity of $\xi_{-4}^{-3/2} d_{16} = 7.5 \nu_{b,14}^{-1} \delta_{50} B_{m,10}^{-3/2}$ (valid for $\beta' = 5/3$; § 2) is self-consistently determined. Making use of equation (5) to eliminate B_m , we have $d = 2.6 \times 10^{16} (\delta_{50} \xi_{-4})^{3/2}$ cm for Φ_2 [$2.4 \times 10^{16} (\delta_{50} \xi_{-4})^{3/2}$ cm for $\Phi_{5/3}$], given the common parameter values (such as $\nu_{b,14} = 2$). To estimate d , here we call for another expression, $\nu_c = 1.0 \times 10^{22} \delta_{50} \xi_{-4}$ Hz [independent of (β, β') ; § 2]. Using this to eliminate $\delta \xi$ from the d -expression, we obtain the simple scaling of $d = 8.2 \times 10^{14} \nu_{c,21}^{3/2}$ cm for Φ_2 ($7.5 \times 10^{14} \nu_{c,21}^{3/2}$ cm for $\Phi_{5/3}$), where $\nu_{c,21} = \nu_c/10^{21}$ Hz. The size d implies the allowable minimum of D ; e.g., $\nu_{c,21} = 0.1 - 10$ (yet involving the large observational uncertainty) provides $D_{16} \gtrsim 10^{-3}$ to 1 (where $D_{16} = D/10^{16}$ cm), as reconciled with the previous results (e.g., Fossati et al. 2000b; Krawczynski et al. 2001; Błażejowski et al. 2005). It also turns out, from the ν_c -scaling, that the range of $\nu_{c,21} < 10^2$ accommodates $\xi \ll 1$, and thereby the assumption of $b \ll 1$ (§ 2).

In addition, given an energy input into the jet, particle density n is estimated. Assuming that electron injection operates at $\gamma_{\text{inj}} \ll \gamma^*|_{\lambda=d} (\leq \gamma^*)$, we approximately get $n \simeq (\kappa/0.6) \gamma_{\text{inj}}^{-0.6}$ (for $p = 1.6$), to find that the steady luminosity of 10^{44} ergs s $^{-1}$, which appears to retain a dominant portion around the ν_b , requires $n \gtrsim 6 \times 10^4 \gamma_{\text{inj}}^{-0.6} D_{16}^{-3} B_{m,10}^{-1.3}$ cm $^{-3}$ (when supposing a spherical emitting volume with the diameter of D). Recalling $B_{m,10} \lesssim 5$, we thus read $n \gtrsim 10^3 D_{16}^{-3}$ cm $^{-3}$ for ordinary $\gamma_{\text{inj}} \sim O(1)$; note that an upper bound can be given by imposing the conditions of, e.g., pair-plasma production ($T \gtrsim 1$ MeV) and radial confinement ($nT \lesssim B_m^2/8\pi$), such that $n \lesssim 10^8$ cm $^{-3}$ (suggesting $D_{16} \gtrsim 10^{-2}$).

In conclusion, the gamma-ray lags of 1 – 2 days measured in Mrk 421 have been nicely reproduced by the hierarchical turbulent model of a jet. The crucial finding is that the structural transition $\Phi_2 \rightarrow \Phi_{5/3}$ results in downshifting the upper bound of the observable lag [in a TeV ($\epsilon_{\gamma,1} \simeq 1$) band] from 2.2 to 1.7 days, in accordance with a closer inspection from 2002 to 2004 by

Błażejowski et al. (2005). A typical 1.8 day lag (in the 2002/2003 season) suggests $\delta = 10 - 92$ and $B_m = 10 - 22$ G (Fig. 3); the latter provides an upper limit of local magnetic intensity. The present model as a possible alternative to the previous leptonic (e.g., Sikora et al. 1994;

Bednarek & Protheroe 1997; Konopelko et al. 2003) and hadronic scenarios (e.g., Mücke & Protheroe 2001) will shed light on puzzling aspects of broadband spectral variability.

REFERENCES

- Aharonian, F. A. 2004, *Very High Energy Cosmic Gamma Radiation* (River Edge: World Scientific)
- Bednarek, W., & Protheroe, R. J. 1997, *MNRAS*, 292, 646
- Błażejowski, M., et al. 2005, *ApJ*, 630, 130
- Catanese, M., & Weekes, T. C. 1999, *PASP*, 111, 1193
- Cui, X. 2004, *ApJ*, 605, 662
- Dermer, C. D., & Schlickeiser, R. 1993, *ApJ*, 416, 458
- Fossati, G., et al. 2000a, *ApJ*, 541, 153
- . 2000b, *ApJ*, 541, 166
- Ghisellini, G., Celotti, A., Fossati, G., Maraschi, L., & Comastri, A. 1998, *MNRAS*, 301, 451
- Honda, M., & Honda, Y. S. 2004, *ApJ*, 617, L37
- . 2007, *ApJ*, 654, 885
- Honda, M., Meyer-ter-Vehn, J., & Pukhov, A. 2000a, *Phys. Plasmas*, 7, 1302
- . 2000b, *Phys. Rev. Lett.*, 85, 2128
- Konopelko, A., Mastichiadis, A., Kirk, J., De Jager, O. C., & Stecker, F. W. 2003, *ApJ*, 597, 851
- Krawczynski, H., et al. 2001, *ApJ*, 559, 187
- Krommes, J. A. 2002, *Phys. Rep.*, 360, 1
- Macomb, D. J., et al. 1995, *ApJ*, 449, L99
- Maraschi, L., Ghisellini, G., & Celotti, A. 1992, *ApJ*, 397, L5
- Medvedev, M. V., & Loeb, A. 1999, *ApJ*, 526, 697
- Montgomery, D., & Liu, C. S. 1979, *Phys. Fluids*, 22, 866
- Mücke, A., & Protheroe, R. J. 2001, *Astropart. Phys.*, 15, 121
- Piner, B. G., et al. 1999, *ApJ*, 525, 176
- Rebillot, P. F., et al. 2006, *ApJ*, 641, 740
- Sembay, S., et al. 2002, *ApJ*, 574, 634
- Sikora, M., Begelman, M. C., & Rees, M. J. 1994, *ApJ*, 421, 153
- Silva, L. O., et al. 2003, *ApJ*, 596, L121
- Takahashi, T., et al. 1996, *ApJ*, 470, L89
- Tavecchio, F., Maraschi, L., & Ghisellini, G. 1998, *ApJ*, 509, 608
- Tramacere, A., Massaro, F., & Cavaliere, A. 2007, *A&A*, 466, 521